C_{60} fragmentation in charge-changing collisions with slow Au^+ ions

Y. Nakai,[1] T. Majima,[2,*] T. Mizuno,[3,†] H. Tsuchida,[3] and A. Itoh[3]
[1] *Radioactive Isotope Laboratory, RIKEN Nishina Center, Wako, Saitama 351-0198, Japan*
[2] *Department of Physics, Tokyo Metropolitan University, Hachioji, Tokyo 192-0397, Japan*
[3] *Department of Nuclear Engineering, Kyoto University, Kyoto 606-8501, Japan*

(Received 8 March 2010; revised manuscript received 9 March 2011; published 12 May 2011)

We investigated ionization and fragmentation of C_{60} in the charge-changing collisions of 2.0 keV/amu Au^+ ions with C_{60} molecules. We performed simultaneous measurements of product ions, the number of secondary electrons, and a charge-selected outgoing Au projectile. The production of C_{60}^+ ions was predominant in the single-electron capture (1-capture) process. In contrast, multifragmentation of C_{60} was predominant in the single-electron loss (1-loss) process. The multifragmentation was enhanced in the 1-loss process compared with the 1-capture process when the same number of electrons was emitted from C_{60}. This enhancement was also observed when a fast Si ion traveled close to a carbon nucleus [T. Majima *et al.*, Phys. Rev. A **74**, 033201 (2006)]. The 1-loss process of slow Au^+ ions is considered to occur closer to a carbon nucleus than does the 1-capture process. Multifragmentation of C_{60} is caused by internal electronic excitation although it is probably assisted by nuclear stopping when, at least, the electronic excitation of C_{60} is small.

DOI: 10.1103/PhysRevA.83.053201 PACS number(s): 36.40.Qv

I. INTRODUCTION

Ionization and fragmentation of isolated C_{60} molecules triggered by photons and charged particles have been extensively studied. Considerable information about the fundamental properties of C_{60}, the unimolecular reaction mechanism, and collision dynamics between the incident particles and C_{60} has been obtained [1–26]. In particular, the information about the charge state, r, of a prefragmented ion C_{60}^{r+} provides insights into collision dynamics and fragmentation after collision. This information has been obtained using the triple-coincidence technique, i.e., by simultaneous measurements of product ions, secondary electrons, and charge-selected outgoing projectiles [14–24]. Notable observations with respect to fast-ion impact are that (i) the multifragmentation of a C_{60} molecule is induced even at small values of r ($r \sim 3$) and (ii) the number of purely ionized electrons (n_i) that are emitted from C_{60} without being captured by an incident ion has a strong correlation with the degree of fragmentation [20–24]. These observations indicate that (i) it is not the Coulomb repulsion but the internal electronic excitation that plays a crucial role in the fragmentation at relatively small values of r and (ii) n_i can be used as a proxy for the degree of internal electronic excitation of a prefragmented C_{60} ion.

In the collision between C_{60} and a heavy ion in a low-charge state, the degree of fragmentation changes with the distance of the projectile trajectory from C_{60}. The projectile ion interacts very weakly with C_{60} at a distant or peripheral collision where a relatively small or no overlap exists between a C_{60} and a projectile ion. In this case, C_{60} is not sufficiently excited and thus cannot disintegrate. With an increase of the overlapped region the effective charge of the projectile, i.e., the "averaged" charge felt by target electrons contributing to electronic stopping, increases because the Coulomb interaction between a projectile nucleus and target electrons is not completely screened by projectile electrons close to a projectile trajectory. Accordingly, the interaction rapidly strengthens with the overlap and prefragmented C_{60} ions are sufficiently excited, resulting in multifragmentation. This trajectory-dependent fragmentation would appear more prominently for low-charged but high-Z (where Z is the atomic number) projectiles with low velocities because the effective projectile charge varies strongly with the projectile trajectory. Therefore, the reaction product distribution in a projectile charge-changing process will reflect the projectile trajectories where the charge-changing process occurs. Moreover, the relationship of the product-ion distribution with r (or n_i) will also provide detailed information on fragment production in charge-changing collisions. Thus far, no investigation has been conducted for such high-Z heavy ions, except for our previous experiments using Au projectiles with a velocity ranging from 0.2. to 1.1 a.u. [25]. However, in Ref. [25] only reaction product distributions were measured and, therefore, detailed information such as the r-distribution of prefragmented C_{60}^{r+} was not obtained.

In the present study, we focus on the ionization and fragmentation of C_{60} in the charge-changing collisions with slow Au^+ ions. Triple-coincidence measurements were performed using slow Au^+ ions at a velocity of 0.28 a.u. (or 2.0 keV/amu) for the single-electron loss (1-loss) and single-electron capture (1-capture) processes. The intensity distributions of fragment ions for loss and capture collisions are compared and the relationship between the degree of fragmentation and the internal excitation of prefragmented C_{60}^{r+} ions is discussed.

II. EXPERIMENT

The present experiment was performed using the QSEC 1.7-MV tandem Cockcroft–Walton accelerator at Kyoto University. Here, we only provide an outline of the experiment

*Present address: Department of Nuclear Engineering, Kyoto University, Kyoto 606-8501, Japan.
†Present address: Photon Factory, Institute of Materials Structure Science, KEK, Tsukuba 305-0801, Japan.

because the experimental method and apparatus have already been described in Refs. [20–23].

An incident beam of 2.0 keV/amu Au^+ was collimated and charge-purified using a magnetic charge selector upstream of the collision chamber. High-purity (99.98%) C_{60} powder was sublimated at 550°C in a temperature-controlled oven. The incident ion and the target C_{60} molecular beams crossed at right angles. The base pressure of the collision chamber was maintained below 3×10^{-6} Pa. After collisions with C_{60} molecules the outgoing projectiles were charge-separated using an electrostatic deflector and detected using a movable surface-barrier semiconductor detector. Positive product ions and secondary electrons were extracted in opposite directions by an electric field applied perpendicular to the direction of the incident beam. The mass-to-charge ratio (m/q) of the product ions was measured by a time-of-flight (TOF) method. The product ions were detected using a two-stage multichannel plate with a front voltage of −4.7 kV. This voltage is sufficient to detect the fragment ions C_n^+ with $n \leqslant 11$ and C_{60}^{r+} ions (for $r \geqslant 3$) with a detection efficiency [12] of approximately unity. The detection efficiencies for the C_{60}^+ and C_{60}^{2+} ions were estimated to be 0.61 and 0.97, respectively, with the method from Ref. [12]. Using these efficiencies, we corrected the yields of the C_{60}^+ and C_{60}^{2+} ions. The secondary electrons were detected using a passivated-implanted-planar-silicon detector (referred to as e^--SSD) biased at +30 kV with an electron-collection efficiency of ∼0.94 [20]. We determined the number of secondary electrons, n_e, emitted in a single collision by analyzing the pulse-height spectra of e^--SSD and taking into account the backscattering effect [20].

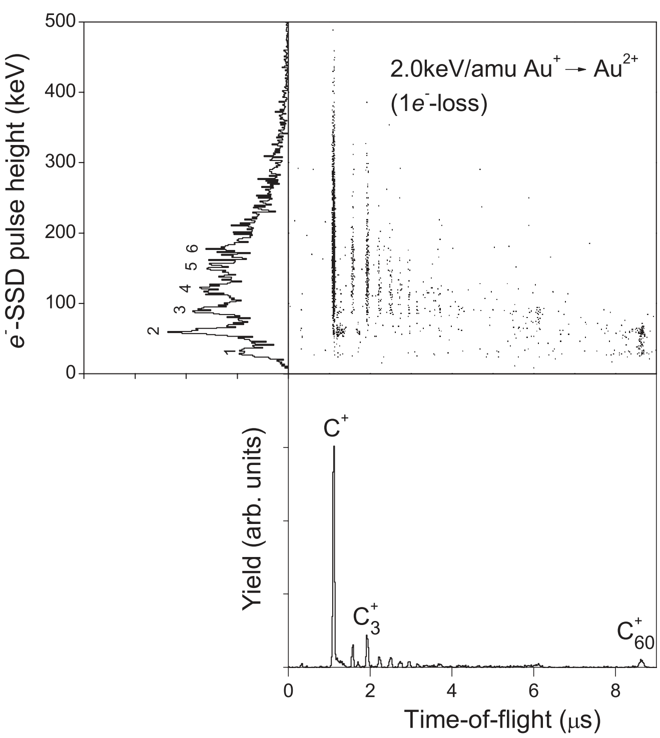

FIG. 1. Two-dimensional coincidence map between TOF and the pulse height of e^--SSD obtained for single-electron loss (1-loss) process. The numbers at the peaks of the SSD pulse indicate the n_e corresponding to each peak.

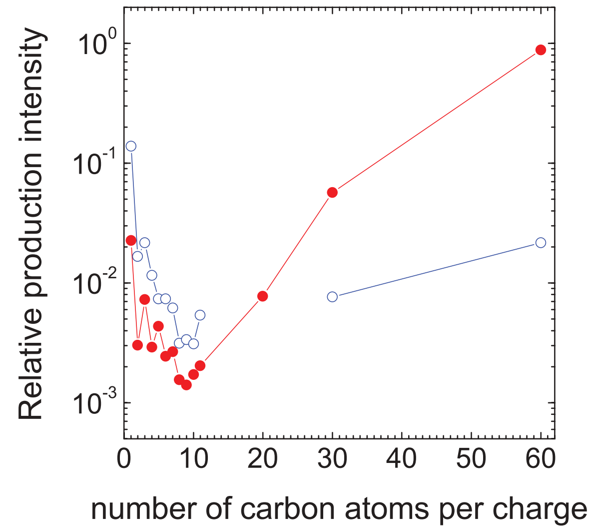

FIG. 2. (Color online) Relative intensity for each product ion in 1-capture (solid circle) and 1-loss (open circle) processes.

Figure 1 shows a two-dimensional coincidence map between TOF and n_e obtained for the 1-loss collisions. The horizontal and vertical axes correspond to TOF of the product ions and the pulse height of e^--SSD, respectively. The charge state, r, of a prefragmented C_{60} ion was determined by $r = n_e - 1$ and $r = n_e + 1$ for the 1-loss and 1-capture processes, respectively. It should be noted that n_e for the 1-loss process includes a lost electron from the projectile ion.

III. EXPERIMENTAL RESULTS

Figure 2 shows the relative production intensities of fragment ions (C_1^+–C_{11}^+) and intact parent ions in the 1-loss and 1-capture processes. C_{60}^+ ion production is predominant in the 1-capture process. This indicates that the 1-capture process mainly occurs in the peripheral collisions with the C_{60} molecules, where the excitation energy of prefragmented C_{60} ions is small owing to the low electron density in the peripheral region of C_{60}. We estimated a critical distance (from the center of C_{60}) of ∼15 a.u. for the 1-capture by the incident Au^+ ion using the classical over-barrier model [6,28] and the well-known ionization potential of C_{60}, 7.6 eV. The obtained critical distance has a value close to that of the outer radius of the C_{60} electron cloud shell, i.e., ∼10 a.u. The electron capture at the periphery of C_{60} is also consistent with other investigations of electron capture using slow, light, and low-charged ions [17,26]; however, it is fairly different from the 1-capture process using slow and highly charged ions [6], whose critical distance is much larger than 10 a.u.

In contrast, a complete disintegration into small fragment ions is predominant in the 1-loss process. The m/q distribution in the 1-loss process is similar to that in the collisions between a 2.0 keV/amu neutral Au atom and a C_{60} [25], where electron loss and non-charge-changing processes of projectiles occur predominantly. The occurrence probability of the 1-loss process is approximately one-fourth of that of the 1-capture process.

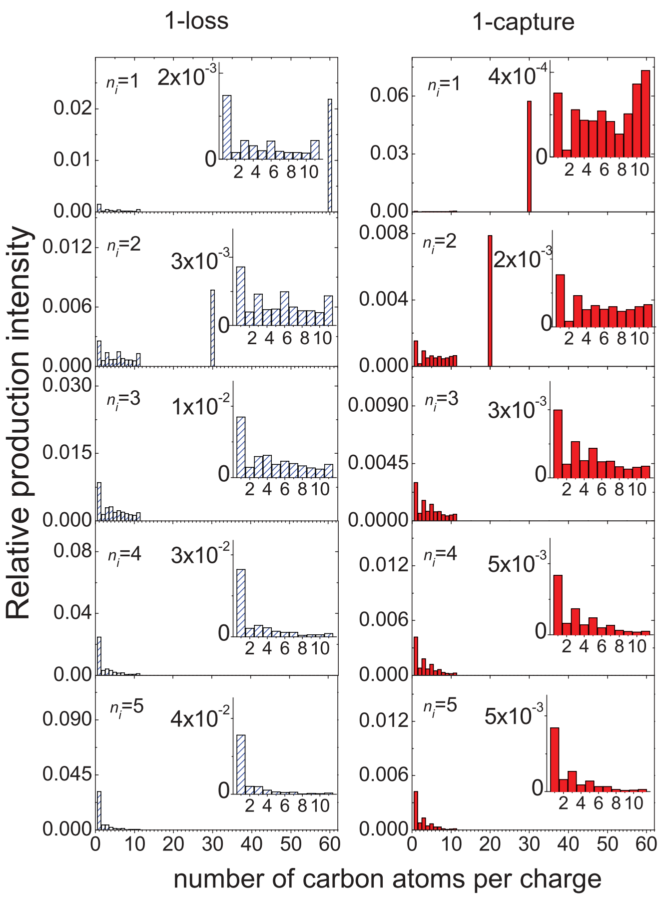

FIG. 3. (Color online) Product-ion distributions for $n_i = 1$–5 in 1-loss (hatched) and 1-capture (filled) processes. The vertical scales for each n_i ($n_i \geqslant 2$) are adjusted so that the relative intensities for C_1^+ are shown with bars of almost the same height. Insets show the distribution from C_1^+ to C_{11}^+ for each n_i.

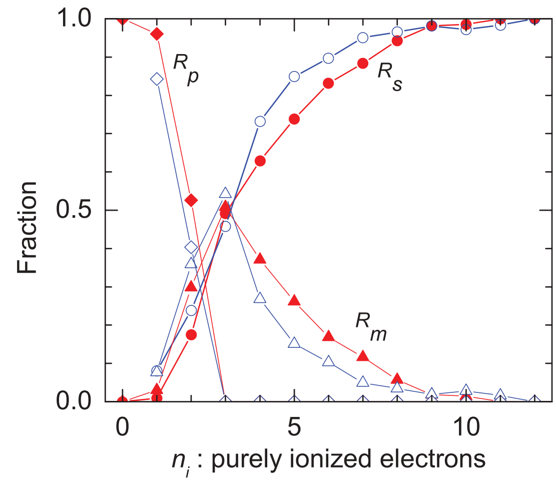

FIG. 4. (Color online) Fractions of intact ions $C_{60}^{1+,2+,3+}$ (rhombus), medium-sized fragment ions C_4^+–C_{11}^+ (triangle), and small fragment ions C_1^+–C_3^+ (circle) in the 1-loss (open symbols) and 1-capture (solid symbols) processes, represented as a function of n_i.

It should be noted that although we detected the 1-loss and 1-capture processes, we were unable to detect the double-electron loss and capture processes in the present experiment, unlike the fast Si^{2+} ion impact cases where the double-electron loss and capture processes could be distinctly measured [21].

Figure 3 shows the relative intensities of the product ions for the number of purely ionized electrons, $n_i = 1$–5, in the 1-loss and 1-capture processes, where n_i is calculated as $n_i = r = n_e - 1$ and $n_i = r - 1 = n_e$, respectively. Small and medium-sized fragment ions (C_1^+–C_{11}^+), which are thought to be produced in multifragmentation, can be observed even at $n_i = 1$ in both processes. However, these fragment-ion distributions for $n_i = 1$ in the 1-loss and 1-capture processes clearly differ from each other, i.e., the enhancement of C_1^+ production is found in the 1-loss process. Small and medium-sized fragment ions become more intense at $n_i = 2$ and dominate at $n_i = 3$ in both the 1-loss and 1-capture processes. Although the intensity distributions for the 1-loss and 1-capture processes become qualitatively similar with increasing n_i, the intensities of small and medium-sized fragment production in the 1-loss process exceeds those of the 1-capture process for all n_i, i.e., transfer ionization leading to multifragmentation in the 1-capture process has a lower probability of occurrence than the target ionization leading to multifragmentation in the 1-loss process for all n_i.

Figure 4 shows the fractions of intact ions ($C_{60}^{1+,2+,3+}$), R_p, medium-sized fragment ions (C_4^+–C_{11}^+), R_m, and small fragment ions (C_1^+–C_3^+), R_s, illustrating the degree of fragmentation more clearly; the degree of fragmentation is higher when R_s is larger and R_p is smaller. These fractions satisfy the relationship $R_p + R_m + R_s = 1$. The intact ions rapidly decrease with n_i and almost disappear at $n_i = 3$. In contrast, the small fragment ions rapidly increase with n_i and become predominant products in both the 1-loss and 1-capture processes in the region of $n_i \gtrsim 5$. Note that a discrepancy in the fractions exists between the 1-loss and 1-capture processes, particularly in the $4 \leqslant n_i \leqslant 7$ region.

IV. DISCUSSION

First, we discuss the fragmentation feature in the region of $n_i \leqslant 7$ in terms of electronic excitation energy of prefragmented C_{60} ions. For the estimation of the internal electronic excitation energy, we used the knowledge that the total energy transferred to the electrons in a target molecule (E_d) is divided among the excited and purely ionized electrons with a certain partition rate, α, on average over impact parameter [3,20–23]. Then, the internal electronic excitation energy $E_{\rm int}$ is given by $E_{\rm int} = (1 - \alpha)E_d$ and the energy transferred to the purely ionized electrons $E_{\rm ion}$ is expressed by $E_{\rm ion} = \alpha E_d$.

In the estimation of α, we assumed that a projectile ion independently interacts with each carbon atom in C_{60}. Then, because α is the value estimated by averaging over impact parameter, it can be approximated as $\alpha = L_i/(L_i + L_e)$, where L_i and L_e are the partial stopping power of projectiles related to the ionization and excitation processes of carbon atoms. However, in the absence of available information about L_i and L_e for the $Au^+ + C$ system, we applied available theoretical findings for H^+ traveling in H_2O vapor with energies ranging from 0.5 to 10^4 keV [27]. The L_i and

L_e values for H^+ in H_2O vapor were calculated using (i) scaling formulas of cross sections for the processes related to ionization and excitation and (ii) equilibrium-charge-state distribution of protons. Thus, in the present study, the partition rate, α, of C_{60} was estimated to be $L_i/(L_i + L_e)$ using L_i and L_e calculated in Ref. [27]. Consequently, at the present velocity of 0.28 a.u. α of C_{60} was estimated to be ∼0.6 and for excited electrons $1 - \alpha \sim 0.4$.

Moreover, the total kinetic energy of the purely ionized electrons, $E_{\rm kin}$, is provided by $E_{\rm ion}$ minus the sum of their ionization potentials (E_p). Then, $E_{\rm kin}$ and E_p are given by $(1-\beta)E_{\rm ion}$ and $\beta E_{\rm ion}$, where β is the division rate. Our recent experimental investigation for the collision of a silicon ion with C_{60} [24] reveals that β increases with a decrease in the projectile velocity and the rate of increasing β per unit rate of decreasing velocity becomes small in the $\lesssim 30$ keV/amu region. We carefully extrapolated β obtained in Ref. [24] and estimated that $\beta \sim 0.4$ at the present velocity.

Using the definition of α and β, $E_{\rm int}$ is expressed by $E_{\rm int} = E_{\rm ion}(1-\alpha)/\alpha = E_p(1-\alpha)/(\alpha\beta)$. Therefore, when we assumed $\alpha = 0.6$ and $\beta = 0.4$ for this collision velocity, $E_{\rm int}$ of a prefragmented C_{60}^{r+} ion was roughly estimated by $E_{\rm int} = E_p \times 0.4/(0.6 \times 0.4)$. The kth ionization potential of $I_k = 3.85 + 3.25k$ eV [28] was used in the estimation of E_p. For the 1-loss process, E_p is estimated as $\sum_{j=1}^{n_i} I_j$. By assuming that the most loosely bound electron is captured by the projectile ion similar to Ref. [19], E_p can be expressed as $E_p = \sum_{j=2}^{n_i+1} I_j$ in the 1-capture process since the energy transferred to a captured electron contributes neither to pure ionization nor to internal electronic excitation. In Table I the estimated values of $E_{\rm int}$ are presented for $n_i = 2$–7. We would like to point out that the fragment patterns for various projectile ions in the MeV region were found to be governed by $E_{\rm int}$ estimated with α and β for each projectile and its velocity [3].

$E_{\rm int}$ values for the 1-loss and 1-capture processes were estimated to be 52 and 68 eV, respectively, at $n_i = 3$, where C_{60} ions almost disappear in the m/q distributions, as shown in Fig. 4. In the case of 2-MeV Si^{2+} impact, C_{60} ions almost disappear at $n_i = 4$ or 5 [20], where $E_{\rm int}$ was estimated to be 48 ($n_i = 4$) and 68 eV ($n_i = 5$), respectively ($\alpha = 0.8$ and $\beta = 0.25$), using I_k from Ref. [28]. These values of $E_{\rm int}$ are roughly in agreement with those at $n_i = 3$ in the present experiment. Furthermore, at $n_i = 5$, where small-sized fragment ions become the dominant products, $E_{\rm int}$ was estimated to be 113 and 140 eV for the 1-loss and 1-capture processes, respectively. These values are consistent with the excitation energy as high as 100 eV, which is required for the small fragment ion production from prefragmented C_{60}^{5+} ions in 6.8 keV $F^{2+} + C_{60}$ collisions [16]. Thus, the dependence of C_{60} fragmentation on n_i in the present experiment is roughly explained by the internal electronic excitation energy, $E_{\rm int}$.

TABLE I. Estimated values of internal electronic excitation energy ($E_{\rm int}$) for each n_i. Each corresponding r (i.e., the charge state of a prefragmented C_{60} ion) is also represented.

n_i	r		$E_{\rm int}$ (eV)	
	1-loss	1-capture	1-loss	1-capture
2	2	3	29	40
3	3	4	52	68
4	4	5	80	102
5	5	6	113	140
6	6	7	152	185
7	7	8	197	235

C_{60}^{r+} ions in the ground and low-excited states, even with relatively high r, are found to be metastable [7,10,29]. The metastability of C_{60}^{r+} ions originates in the potential barrier on the fragment paths. Therefore, it should be confirmed that the internal energy is high enough to trigger the fragmentation of the prefragmented C_{60}^{r+} ions. According to Ref. [29], the potential barrier in the charged C_2 emission from C_{60}^{r+} decreases with r; the values for $r = 3$ and 8 are 9.9 and 7.6 eV, respectively. The potential barrier experimentally estimated for the process of $C_{60}^{r+} \to C_{58}^{(r-1)+} + C_2^+$ also decreases with r from ∼11 eV ($r = 3$) to ∼4 eV ($r = 8$) [7,10,15]. These potential barriers are much smaller than the estimated $E_{\rm int}$, especially for $n_i \geqslant 3$ where the intact ions disappear. This indicates that the internal excitation overcomes the potential barrier and triggers fragmentation of C_{60}^{r+} ions.

As mentioned above, the degree of fragmentation in the 1-loss process was higher than in the 1-capture process at the same n_i. In the case of 2-MeV Si^{2+} impact, a minimal difference was observed between the 1-loss and 1-capture processes [20]. In contrast, a discrepancy was observed in the double-electron loss process where the fraction R_s at a large scattering angle (i.e., small impact parameter from a carbon nucleus) was found to be larger than at a small scattering angle (i.e., large impact parameter) [21]. Moreover, one of our investigations on the scattering-angle dependence using 2-MeV C^+ ions indicated that the production probability for a specific fragment ion strongly depends on the distance of the projectile trajectory from a carbon-nuclear shell (or more precisely, a carbon nucleus) of C_{60}; smaller fragment ions are produced during collisions closer to a carbon-nuclear shell [23]. Therefore, the discrepancy of the fragment degree observed here is considered to reflect the difference between the projectile-trajectory distributions in the 1-loss and 1-capture processes for the same n_i. The discrepancy, specifically, indicates that the 1-loss process occurs in collisions closer to a carbon nucleus than the 1-capture process, even when the same n_i electrons are purely ionized. In the collisions with the projectile trajectories close to a carbon nucleus (i.e., close collision), the electronic excitation is expected to shift toward a higher region because the projectile ions travel in the high-electron-density region near the carbon nuclei. In such a case, the actual electronic excitation in the 1-loss process is thought to be much higher than that estimated without considering the projectile trajectory dependence.

In close collisions, we also expect the influence of nuclear stopping owing to the screened Coulomb interaction between Au^+ and a carbon atom. To clearly observe nuclear stopping by excluding electronic excitation, it may be appropriate to examine the fragment distributions at small values of n_i, e.g., $n_i = 1$ or 2, because of the strong positive correlation between internal electronic excitation and n_i as described above and in Refs. [20–24], although multifragmentation for small values of n_i is not a dominant process. As shown in Fig. 3, an enhancement of C_1^+ production was found in the 1-loss process at $n_i = 1$. This enhancement may be induced by a knock-on process in close collisions, as was interpreted for C_1^+ production observed for the slow Ar^+ impact [19]. Thus, for $n_i = 1$, the nuclear-stopping effect may be observed in the present study, as is expected in slow collisions with extremely heavy ions [25].

The knock-on process was also investigated in the collision of an accelerated C_{60} ion with a rare-gas atom (He, Ne, Ar) [4,9] in advancement of the slow Ar^+ impact experiment in Ref. [19]. It was shown that the binary collision of a rare-gas atom with a carbon atom in C_{60}^+ is important to explain the experimental information on the knock-on process, e.g., fragment-mass distributions and the formation probability of residual C_{59}^+. In view of the importance of the binary collision, we estimated the critical impact parameter, b_c, from a carbon nucleus in order to compare the present experiment with the previous studies [4,9,19]. The b_c value is estimated at the point where the recoil energy of a carbon atom matches with the knock-on threshold energy of 13.5 eV [30]. According to Ref. [4], the knock-on process is assumed to occur at an impact parameter less than b_c. In the present estimation of b_c, the Moliére potential was adopted. The value of b_c for 400-keV Au^+ was estimated to be 1.5 a.u., whereas for Ne under the experimental conditions in Refs. [4,9] the estimate was 1.6 a.u.. For the Ar^+ ions at 7, 14, and 20 keV in Ref. [19] b_c was also estimated to be 1.6, 1.4, and 1.3 a.u., respectively. Thus, the b_c value for 400-keV Au^+ is comparable to those of the previous studies where the knock-on process was observed. Therefore, it is reasonable that the knock-on process is observed in the collisions of 400-keV Au^+ with C_{60}. The multiple knock-on of carbon atoms suggested by the simulation for Ne-C_{60}^+ collisions [9] might also occur in the present case. Note that the b_c value of 1.5 a.u. in the present case is as small as the expectation value of the 5d-orbital radius of a gold atom (which is the outermost orbital of a Au^+ ion and is equal to 1.5 a.u.) [31].

Here, we briefly speculate on the mechanism of removing an electron with a binding energy $\geqslant$ 20.5 eV from Au^+ (since the ionization potential of Au^+ is 20.5 eV). At a velocity equal to 0.28 a.u., the outer shell (5d) electrons of a Au^+ ion form quasi-molecular orbitals with the valence electrons of a C_{60} molecule during collision. With decreasing internuclear distance some orbitals can be promoted to higher energies; this is the so-called electron promotion mechanism [32]. This mechanism is known to account well for inner shell excitation in ion-atom collisions, and it may also account for the ionization of outer d-shell electrons with high binding energies [33]. It is inferred that the electron promotion occurring close to a carbon nucleus is one of the important projectile electron-loss mechanisms in the region with a collision velocity of 0.28 a.u.

V. SUMMARY

We performed triple-coincidence measurements to investigate the ionization and fragmentation of C_{60} for the 1-capture and 1-loss processes in the collisions of 2.0 keV/amu Au^+ ions with C_{60}. The intensity of the 1-capture process was found to be approximately four times larger than that of the 1-loss process. The C_{60}^+ ion production was predominant in the 1-capture process. In contrast, the multifragmentation of C_{60} was predominant, and also enhanced for the same n_i, in the 1-loss process. This enhancement was also observed in close collisions with fast Si ions [21]. Therefore, it is considered that the 1-loss process occurs closer to a carbon nucleus than the 1-capture process when the same number of electrons is purely ionized. It is believed that internal electronic excitation is more significant than nuclear stopping for multifragmentation in the slow collision of C_{60} with Au^+ ions. It is still unclear how nuclear stopping aids fragmentation in close collision [25]: however, when $n_i = 1$ at least, the knock-on process appears to influence the fragmentation in close collision.

ACKNOWLEDGMENTS

We thank K. Yoshida, K. Norizawa, and M. Naitoh for their technical support during this experiment.

[1] E. E. B. Campbell and F. Rohmund, Rep. Prog. Phys. **63**, 1061 (2000), and references therein.
[2] P. Scheier and T. D. Mark, Phys. Rev. Lett. **73**, 54 (1994).
[3] H. Tsuchida, A. Itoh, K. Miyabe, Y. Bitoh, and N. Imanishi, J. Phys. B **32**, 5289 (1999).
[4] M. C. Larsen, P. Hvelplund, M. O. Larson, and H. Shen, Eur. Phys. J. D **5**, 283 (1999).
[5] J. U. Andersen, P. Hvelplund, S. B. Nielsen, U. V. Pedersen, and S. Tomita, Phys. Rev. A **65**, 053202 (2002).
[6] H. Cederquist *et al.*, Phys. Rev. A **61**, 022712 (2000).
[7] H. Cederquist, J. Jensen, H. T. Schmidt, H. Zettergren, S. Tomita, B. A. Huber, and B. Manil, Phys. Rev. A **67**, 062719 (2003).
[8] S. Tomita, J. U. Andersen, C. Gottrup, P. Hvelplund, and U. V. Pedersen, Phys. Rev. Lett. **87**, 073401 (2001).
[9] S. Tomita, P. Hvelplund, S. B. Nielsen, and T. Muramoto, Phys. Rev. A **65**, 043201 (2002).
[10] S. Tomita, H. Lebius, A. Brenac, F. Chandezon, and B. A. Huber, Phys. Rev. A **67**, 063204 (2003).
[11] Y. Nakai, T. Kambara, A. Itoh, H. Tsuchida, and Y. Yamazaki, Phys. Rev. A **64**, 043205 (2001).
[12] A. Itoh, H. Tsuchida, T. Majima, and N. Imanishi, Phys. Rev. A **59**, 4428 (1999).
[13] U. Kadhane, A. Kelkar, D. Misra, A. Kumar, and L. C. Tribedi, Phys. Rev. A **75**, 041201 (2007).
[14] S. Martin, L. Chen, A. Denis, R. Brédy, J. Bernard, and J. Désesquelles, Phys. Rev. A **62**, 022707 (2000).

[15] S. Martin, L. Chen, R. Brédy, J. Bernard, M. C. Buchet-Poulizac, A. Allouche, and J. Désesquelles, Phys. Rev. A **66**, 063201 (2002).
[16] S. Martin, L. Chen, A. Salmoun, B. Li, J. Bernard, and R. Bredy, Phys. Rev. A **77**, 043201 (2008).
[17] S. Martin, L. Chen, J. Bernard, R. Bredy, M. C. Buchet-Poulizac, X. Ma, and B. Wei, Europhys. Lett. **74**, 985 (2006).
[18] L. Chen, S. Martin, J. Bernard, and R. Bredy, Phys. Rev. Lett. **98**, 193401 (2007).
[19] L. Chen, B. Wei, J. Bernard, R. Bredy, and S. Martin, Phys. Rev. A **71**, 043201 (2005).
[20] T. Majima, Y. Nakai, H. Tsuchida, and A. Itoh, Phys. Rev. A **69**, 031202 (2004).
[21] T. Majima, Y. Nakai, T. Mizuno, H. Tsuchida, and A. Itoh, Phys. Rev. A **74**, 033201 (2006).
[22] T. Mizuno, T. Majima, Y. Nakai, H. Tsuchida, and A. Itoh, Nucl. Instrum. Methods Phys. Res. B **256**, 101 (2007).
[23] T. Mizuno, D. Okamoto, T. Majima, Y. Nakai, H. Tsuchida, and A. Itoh, Phys. Rev. A **75**, 063203 (2007).
[24] T. Mizuno, H. Tsuchida, T. Majima, Y. Nakai, and A. Itoh, Phys. Rev. A **78**, 053202 (2008).
[25] T. Majima, A. Yogo, F. Obata, H. Tsuchida, Y. Nakai, and A. Itoh, Nucl. Instrum. Methods Phys. Res. B **193**, 209 (2002).
[26] A. Rentenier *et al.*, Phys. Rev. Lett. **100**, 183401 (2008).
[27] J. H. Miller and A. E. S. Green, Radiat. Res. **54**, 343 (1973).
[28] H. Zettergren, H. T. Schmidt, P. Reinhed, H. Cederquist, J. Jensen, P. Hvelplund, S. Tomita, B. Manil, J. Rangama, and B. A. Huber, Phys. Rev. A **75**, 051201 (2007).
[29] S. Díaz-Tendero, M. Alcami, and F. Martin, J. Chem. Phys. **123**, 184306 (2005).
[30] E. S. Parilis, Nucl. Instrum. Methods Phys. Res. B **88**, 21 (1994).
[31] S. L. Saito, At. Data Nucl. Data Tables **95**, 836 (2009).
[32] U. Fano and W. Lichten, Phys. Rev. Lett. **14**, 627 (1965).
[33] The electron promotion of the 4*d*-shell electrons in silver atoms is considered to be one of the prompt-surface-excitation processes in keV ion bombardment of the silver metal surface; see A. Duvenbeck, O. Weingart, V. Buss, and A. Wucher, New J. Phys. **9**, 38 (2008).